

# String Breaking in a 2 + 1D $\mathbb{Z}_2$ Lattice Gauge Theory

Umberto Borla<sup>1</sup>,<sup>\*</sup> Jesse J. Osborne<sup>2</sup>, Sergej Moroz<sup>3,4</sup> and Jad C. Halimeh<sup>5,6,7,\*</sup>

<sup>1</sup>Racah Institute of Physics, The Hebrew University of Jerusalem, Givat Ram, Jerusalem 91904, Israel

<sup>2</sup>School of Mathematics and Physics, The University of Queensland, St. Lucia, QLD 4072, Australia

<sup>3</sup>Department of Engineering and Physics, Karlstad University, Karlstad, Sweden

<sup>4</sup>Nordita, Stockholm University and KTH Royal Institute of Technology, 10691 Stockholm, Sweden

<sup>5</sup>Max Planck Institute of Quantum Optics, 85748 Garching, Germany

<sup>6</sup>Department of Physics and Arnold Sommerfeld Center for Theoretical Physics (ASC), Ludwig Maximilian University of Munich, 80333 Munich, Germany

<sup>7</sup>Munich Center for Quantum Science and Technology (MCQST), 80799 Munich, Germany

(Dated: January 31, 2025)

String breaking is an intriguing phenomenon crucial to the understanding of lattice gauge theories (LGTs), with strong relevance to both condensed matter and high-energy physics (HEP). Recent experiments investigating string breaking in 2 + 1D (two spatial and one temporal dimensions) LGTs motivate a thorough analysis of its underlying mechanisms. Here, we perform matrix product state (MPS) simulations of string breaking in an experimentally relevant 2 + 1D  $\mathbb{Z}_2$  LGT in the presence of two external charges. We provide a detailed description of the system in the confined phase, highlight a number of mechanisms which are responsible for string breaking, and argue that magnetic fluctuations have a stabilizing effect on the strings. Moreover, we show that deep in the confined regime the problem is dual to one-dimensional free fermions hopping on an open chain. Our work elucidates the microscopic processes of string breaking in 2 + 1D LGTs, and our findings can be probed on current superconducting-qubit quantum computers.

**Introduction.**—Gauge theories lie at the heart of the Standard Model of particle physics [1]. They describe the interactions between elementary particles as mediated by gauge bosons [2], and are used to analyze measurements at dedicated particle colliders [3]. Their lattice manifestation, LGTs, have enabled non-perturbative calculations of quantum chromodynamics (QCD), giving insights into the nature of quark confinement [4]. Although initially formulated for high-energy physics (HEP), their usefulness has extended to condensed matter [5–7] as well as quantum many-body physics [8–12]. Recently, there has also been a concerted effort to realize LGTs on quantum hardware [13–23], with the long-term goal of creating a complementary venue for probing HEP phenomena [24–34].

In particular,  $\mathbb{Z}_2$  LGT [5] has emerged as a paradigmatic model for studying phenomena relevant to HEP, condensed matter, and quantum many-body physics. When coupled with dynamical matter, the Ising gauge theory recently shed new light on various physical phenomena such as confinement [35–41], exotic phase transitions [42–47], the Higgs mechanism [48, 49] and constrained quantum dynamics [50–52]. Importantly,  $\mathbb{Z}_2$  LGTs have recently been experimentally realized on quantum simulators in one [53, 54] and two [55, 56] spatial dimensions. Of particular current interest in quantum simulation experiments of  $\mathbb{Z}_2$  LGTs is string-breaking dynamics [54, 55], which has also recently been experimentally observed in U(1) LGTs [57–59]. String breaking is a paradigmatic HEP phenomenon intimately related to confinement in QCD [60, 61]. Upon spatially separating two quarks, the energy stored in the string connecting them becomes large enough to initiate quark-

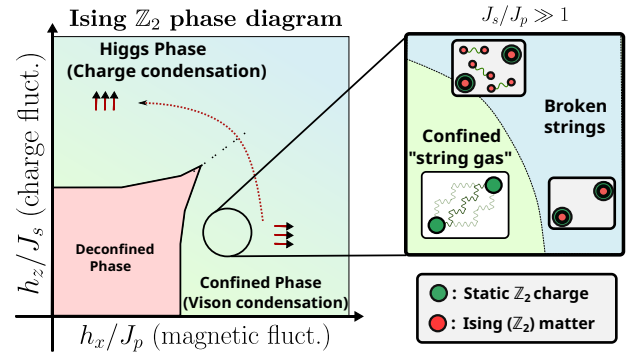


FIG. 1. Left: quantum phase diagram of the model described by Eq. (1). The general characterization of the phases does not change when two static charges are present, but we can now distinguish different regimes depending on whether  $\mathbb{Z}_2$  electric strings are broken. Right: zooming in on the confined region of the phase diagram, we can distinguish different regimes depending on the behavior of strings. As described in the main text, string breaking can be driven by increasing the strength of either external field, but also by decreasing the strength of the magnetic field.

pair creation between them, thereby breaking the string. It is worth noting that string breaking is also a topic of significant interest in condensed matter [62–64].

In the Google Quantum AI experiment [55], a 2 + 1D  $\mathbb{Z}_2$  LGT, equivalent to the toric code with two external fields [65–68], was used to study string dynamics on a superconducting-qubit quantum computer. By fixing the star and plaquette terms to equal strength, they probed the dynamics of strings formed by creating spatially separated local excitations on top of a prepared ground state.

Depending on the degree of confinement manifest in the strength of one of the external field terms, three different regimes of string dynamics were observed. Whereas in the deconfined phase the string is quite dynamic and fluctuates all over the lattice, in the confined phase a more nuanced picture emerges. At weak confinement, the string fluctuations in the transverse direction are strong, while at larger confinement, they are frozen.

In this Letter, we employ the density matrix renormalization group technique (DMRG) [69] to investigate string breaking in this 2 + 1D  $\mathbb{Z}_2$  LGT deep within the confined phase; see Fig. 1. In this regime, where charges are connected by strings of minimal length, we provide a detailed account of string-breaking phenomena that result from a number of different mechanisms. We also show how the presence of a weak magnetic field allows an exact mapping to hopping fermions on an open one-dimensional chain.

**Model.**—We focus on the 2 + 1D  $\mathbb{Z}_2$  LGT on a square lattice, which is the model realized in the recent **Google Quantum AI** experiment [55]. It is described by the Hamiltonian [65]

$$\hat{H} = -J_s \sum_{\mathbf{r}} \hat{\tau}_{\mathbf{r}}^z - J_p \sum_{\mathbf{r}^*} \hat{B}_{\mathbf{r}^*} - h_z \sum_{\mathbf{r}, \eta} \hat{\tau}_{\mathbf{r}}^x \hat{\sigma}_{\mathbf{r}, \eta}^z \hat{\tau}_{\mathbf{r}+\eta}^x - h_x \sum_{\mathbf{r}, \eta} \hat{\sigma}_{\mathbf{r}, \eta}^x, \quad (1)$$

where  $\hat{\tau}_{\mathbf{r}}^z$  represents the matter particle-number operator on site  $\mathbf{r}$  with  $J_s$  the chemical potential, and  $\hat{\sigma}_{\mathbf{r}, \eta}^{x(z)}$  is the electric (gauge) field operator on the link emanating from site  $\mathbf{r}$  in the direction  $\eta$ , with  $h_x$  the electric-field strength. The plaquette operator  $\hat{B}_{\mathbf{r}^*} = \prod_{b \in \square_{\mathbf{r}^*}} \hat{\sigma}_b^z$  with strength  $J_p$ , where the index  $\mathbf{r}^*$  labels the sites of a dual lattice formed by the centers of the plaquettes. The three-body term in Hamiltonian (1) describes gauge-matter coupling with strength  $h_z$ . We also define the star (or vertex) operator  $\hat{A}_{\mathbf{r}} = \prod_{\eta \in +_{\mathbf{r}}} \hat{\sigma}_{\mathbf{r}, \eta}^x$ , the product of  $\hat{\sigma}^x$  on the four links connecting at the vertex  $\mathbf{r}$ . The Hamiltonian (1) is invariant under the set of local gauge transformations  $\hat{G}_{\mathbf{r}} = \hat{A}_{\mathbf{r}} \hat{\tau}_{\mathbf{r}}^z$ , which relates the  $\mathbb{Z}_2$  electric lines, i.e., links where  $\sigma^x = -1$ , emanating from a site to the  $\mathbb{Z}_2$  charge on the same site. Physical states satisfy Gauss's law:  $\hat{G}_{\mathbf{r}}|\psi\rangle = Q_{\mathbf{r}}|\psi\rangle$ , where  $Q_{\mathbf{r}} = \pm 1$  denotes the absence or presence of a static background  $\mathbb{Z}_2$  charge on that particular site. The Hilbert space separates into an exponential number of sectors, each determined by a different distribution of background charges. In order to satisfy Gauss's law, a basis of physical gauge-invariant states must be formed by connecting  $\mathbb{Z}_2$  charges, either dynamical or static, with electric strings. In the following, we will focus on the case where there are two static charges at sites  $\mathbf{r}_1$  and  $\mathbf{r}_2$  ( $Q_{\mathbf{r}_1} = Q_{\mathbf{r}_2} = -1$ ,  $Q_{\mathbf{r} \neq \mathbf{r}_1, \mathbf{r}_2} = +1$ ), and study the properties of the ground state and of the strings connecting them in different regimes.

By fixing the gauge sector, matter degrees of freedom can be integrated out of Hamiltonian (1). The model then reduces to the toric code in a tilted field [70]

$$\hat{H} = -J_s \sum_{\mathbf{r}} Q_{\mathbf{r}} \hat{A}_{\mathbf{r}} - J_p \sum_{\mathbf{r}^*} \hat{B}_{\mathbf{r}^*} - h_z \sum_{\mathbf{r}, \eta} \hat{\sigma}_{\mathbf{r}, \eta}^z - h_x \sum_{\mathbf{r}, \eta} \hat{\sigma}_{\mathbf{r}, \eta}^x, \quad (2)$$

which involves only gauge-invariant link variables. The first term, which includes the static charges, is obtained by solving Gauss's law to yield  $\hat{\tau}_{\mathbf{r}}^z = Q_{\mathbf{r}} \hat{A}_{\mathbf{r}}$ . While it has been appreciated recently that the models (1) and (2) differ in some aspects that involve physical boundaries and entanglement cuts [49, 71], in this paper we do not investigate such aspects. For all our numerical simulations, we use Hamiltonian (2).

In the absence of the external fields  $h_{x,z}$ , Hamiltonians (1) and (2) are invariant under magnetic (electric) one-form symmetries generated by Wilson ('t Hooft) loops. Additionally, the model exhibits an electric-magnetic duality that amounts to exchanging the roles of the star and plaquette operators and redefining the couplings accordingly. For  $J_s = J_p = 1$ , this results in the phase diagram in Fig. 1 being symmetric under reflections with respect to the main diagonal. We note that the placement of static charges breaks this duality, unless one also flips the sign of  $J_p$  on the relevant plaquettes.

The ground-state phase diagram, in the absence of external charges, is well known. A detailed analysis is already present in the seminal paper of Fradkin and Shenker [65], while subsequent studies using Monte Carlo [70, 72] and tensor network [47] techniques highlighted a number of more subtle properties in the vicinity of the critical points. As shown in Fig. 1, there are only two distinct bulk phases. For low values of the external fields, the gauge fields are deconfined, both charge and magnetic fluctuations are inhibited, and the ground state approaches the one of the toric code, exhibiting  $\mathbb{Z}_2$  topological order. At strong external fields, on the other hand, there is a single phase of matter as large values of  $h_x$  and  $h_z$  force a paramagnetic state along a direction determined by their relative strength. In physical terms, however, it is useful to identify two different regimes which are only separated by a smooth crossover. In the electrically dominated phase charges are confined and magnetic excitations (visons) condense. For fixed "chemical potential"  $J_s$  and large  $h_x$  the ground state has no electric strings and no dynamical  $\mathbb{Z}_2$  charges. If static charges are present, these are neutralized by dynamical ones to maintain the no-string condition. In the Higgs regime (large  $h_z$ ), on the other hand, visons are confined and charges condense.

In the absence of dynamical matter, the model reduces to a pure  $\mathbb{Z}_2$  LGT. This limit can be obtained by suppressing matter fluctuations ( $h_z = 0$ ) and by penalizing

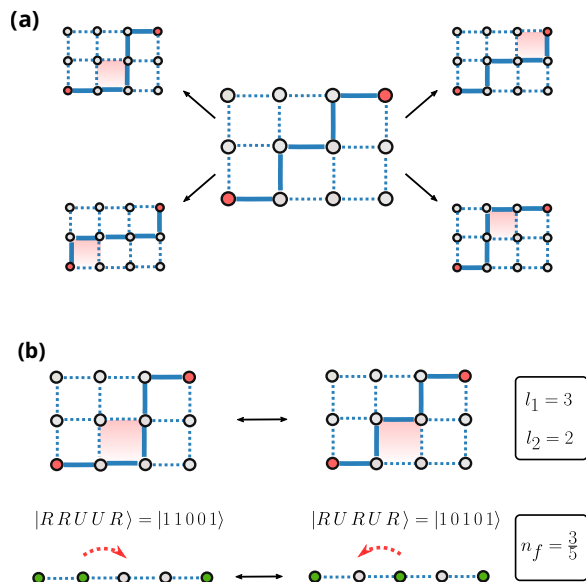


FIG. 2. (a) On a  $3 \times 2$  rectangular patch with static charges at the opposite corners (sites marked in red), 10 string configurations of minimal length  $l = 5$  are possible. At the center, we show the string with the maximum number of corners. In the presence of a plaquette term, this string can resonate with the four other displayed string configurations. Transitions are caused by the action of the operator  $\hat{B}_{\mathbf{r}^*}$  on each of the shaded plaquettes. (b) Mapping between a system of shortest strings and one-dimensional fermions. The transitions between string configurations that are connected by a single application of  $\hat{B}_{\mathbf{r}^*}$  correspond to the nearest-neighbor hopping of a fermion. The fermion filling is fixed to  $l_1/(l_1 + l_2)$ .

occupancy with a large “chemical potential”  $J_s$ . In this scenario the potential between static  $\mathbb{Z}_2$  charges is known [73]. In the deconfined phase, the charges are expected to attract each other via an exponentially decaying potential. In the confined phase, on the other hand, the attractive potential grows linearly with the distance and is equal to the energy cost of the shortest possible string connecting the charges. At the quantum critical point separating the two phases, which lies in the Ising\* universality class, the interaction potential is expected to follow a  $1/R$  power-law behavior [74]. Once dynamical matter is introduced the potential between charges can be screened by  $\mathbb{Z}_2$  charged particles, leading to string breaking phenomena. In the limit of infinite string tension  $h_x \rightarrow \infty$ , particles will occupy the sites where the static charges are to completely neutralize them.

**String phenomenology in the confined phase.**—

We now focus on the phenomenology of strings in the confined phase,  $h_x/J_p \gg h_z/J_s$ . Sufficiently deep in the confined phase, the electric lines connecting the two static charges have a high energy cost proportional to their length, and must therefore be as short as possible. On a square lattice, unless the two charges are in-line, the shortest possible string connecting them is not unique

and, in general, the ground state of the system consists of a superposition of all possible shortest strings.

In the presence of a weak magnetic term, the actual ground-state configuration can be determined by regarding  $J_p$  as a small perturbation. Whenever a string forms a corner, it can resonate with another string of the same length through the application of a plaquette operator  $\hat{B}_{\mathbf{r}^*}$  on that specific corner; see Fig. 2. Since the resonance will lower the ground state energy, strings with the largest number of resonances should appear with a larger weight in the superposition. As the number of available resonances corresponds to the number of corners, the perturbation favors the formation of strings with a “zigzag” structure. Given a rectangular patch of size  $l_1 \times l_2$ , each string configuration connecting the bottom left and top right corners can be obtained by moving horizontally  $l_1$  times and vertically  $l_2$  times, in any order. The string configurations are therefore in one-to-one correspondence with the  $\binom{l_1+l_2}{l_1} = \binom{l_1+l_2}{l_2}$  permutations of the tuple

$$\underbrace{(1, 1, \dots, 1)}_{l_1 \text{ times}}, \underbrace{(0, 0, \dots, 0)}_{l_2 \text{ times}}, \quad (3)$$

where 1 represents a horizontal move and 0 a vertical move. In this framework, transitions between strings correspond to swaps of neighboring pairs of 1 and 0, i.e., a southeast corner represented by  $(0, 1)$  is changed to a northwest corner represented by  $(1, 0)$ . But this is exactly the behavior of  $N = l_1$  nearest-neighbor-hopping fermions on an open chain of length  $L = l_1 + l_2$ , with 1 labeling a site occupied by a fermion and 0 an empty site. Swapping the roles of  $l_1$  and  $l_2$  would correspond to simulating the equivalent system of holes, with identical results due to particle-hole symmetry. The plaquette strength  $J_p$  plays the role of hopping parameter.

What is the leading effect of a weak matter coupling  $h_z$ ? It is straightforward to demonstrate that the matter coupling  $h_z$  does not split the energies of the shortest strings at second order in perturbation theory. At fourth order, it generates the plaquette term perturbatively, which leads to renormalization of the fermion hopping.

As a result of this mapping, deep in the confined regime the ground state of the string is a free Fermi gas of one-dimensional fermions occupying an open chain of length  $L$  at the filling fraction  $l_1/(l_1 + l_2)$ . This picture also allows us to determine string excitations. These correspond, in fact, to the familiar particle-hole pairs in the Fermi gas.

**Numerical study of string breaking.**—In this section we present the results of numerical DMRG simulations carried out with the tensor network Python library TeNPy [75, 76]. This method returns a controlled approximation of the ground state of the system in the form of a matrix product state (MPS) [69]. While the algorithm was originally devised to handle 1 + 1D systems,

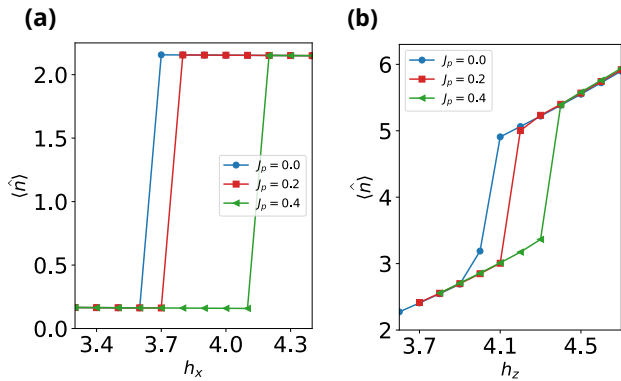


FIG. 3. String breaking driven by directly increasing the energy cost of the (a) electric string and (b) charge (pair) fluctuations. As a figure of merit, we compute the total number of particles in the system, which experiences a sharp jump  $\Delta n = 2$  when a pair forms and neutralizes the static background. In both cases, a finite magnetic coupling  $J_p$  stabilizes the strings, shifting the breaking point to the right. The numerical simulations are performed on cylinders of length  $L_x = 30$  and circumference  $L_y = 6$ . The charges are placed in the central section to avoid boundary effects, at a horizontal distance  $l_x = 5$  and vertical distance  $l_y = 3$ . The star coupling is  $J_s = 15$ , while we fix  $h_z = 1$  and  $h_x = 3$  in panels (a) and (b), respectively.

it is readily adapted to  $2 + 1$ D cylindrical geometries by defining an ordering of sites and treating the cylinder as a winding chain. This has the drawback of artificially introducing long-range interactions, which cause an exponential growth in the virtual dimension of the MPS needed to reach a given accuracy. This limits the circumference sizes that can be reliably simulated. To make our analysis as close as possible to the  $2 + 1$ D limit while retaining good numerical accuracy, we consider a cylinder with  $L_x = 30$  and  $L_y = 6$ , and focus on its central section where the two charges are placed at the opposite corners of a patch of size  $l_1 \times l_2$ , with  $l_1 = 5$  and  $l_2 = 3$ . This mitigates finite-size effects. For this setup, we scan different ranges of parameters to unveil all possible mechanisms that lead to string breaking, and to clarify the physical role of the three independent couplings  $h_x$ ,  $h_z$  and  $J_p$ .

At  $J_p = h_z = 0$ , the Hamiltonian is classical and whether unbroken strings exist depends solely on the energetic competition between the star and electric terms. The cost of a string connecting the two charges is  $\Delta E_s = 2h_x l$ , where  $l = l_1 + l_2$  is the total length of the string. On the other hand, a broken string comes at the cost  $\Delta E_b = 4J_s$  of creating two particles that neutralize static charges. In this simple scenario, therefore, string breaking occurs once the critical string tension  $h_x^* = 2J_s/l$  is reached. This is also confirmed in the presence of small quantum fluctuations generated by the plaquette term, as shown in Fig. 3a.

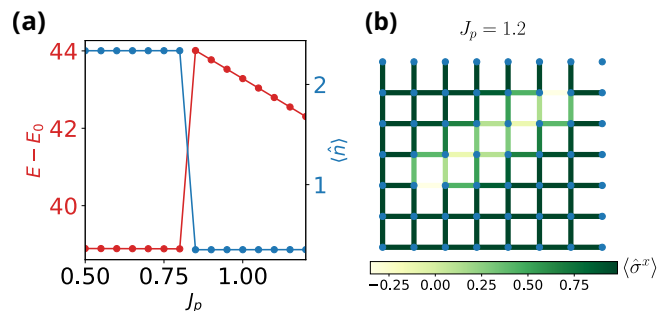


FIG. 4. String breaking can be driven by decreasing the plaquette strength  $J_p$ . (a) The string breaking point is signaled by a sudden jump in the energy and particle number, caused by the creation of two charges that neutralize the static  $\mathbb{Z}_2$  background, which lowers the ground-state energy. (b) Expectation values of  $\hat{\sigma}^x$  in the unbroken string phase. One can see that the two charges are connected by a superposition of strings. The pattern predicted in the main text is clearly recognizable, with the zigzag strings having a higher weight in the superposition. The simulation is done on a cylinder of length  $L_x = 30$  and circumference  $L_y = 6$ , for  $h_x = 3$ ,  $h_z = 1$ , and  $J_s = 10$ .

Next, we consider the possibility of triggering string breaking by increasing the strength of particle fluctuations, determined by the  $h_z$  field. To test this, we start from the same configuration as above with stable unbroken strings and increase  $h_z$ . As shown in Fig. 3b, the strings break for large values of  $h_z$ . In contrast to the electric coupling-driven breaking, this phase is characterized by strong charge fluctuations. Indeed, larger values of  $h_z$  facilitate matter creation, thereby destabilizing strings.

Finally, it is important to understand how a finite plaquette term affects the string breaking. Interestingly, as shown in Fig. 3, we find that the magnetic term has a stabilizing effect on the strings, leading to an increase in the critical values  $h_x^*$  and  $h_z^*$  of the external fields at which strings break. This makes sense because, as described above,  $J_p$  is responsible for string resonances that lower the energy of the system. Following the same logic, we expect that string breaking can occur by *lowering* the plaquette coupling. This is confirmed by the parameter scan presented in Fig. 4, which shows a broken-string regime for low values of the coupling  $J_p$ . Starting at large values of  $J_p$ , we find that the ground-state energy of the system with static charges steadily increases with respect to that in the homogeneous sector where no static charges are present ( $Q_{\mathbf{r}} = +1, \forall \mathbf{r}$ ). However, below a critical value  $J_p^*$ , the string breaks, indicated by the sudden jump in matter occupation by 2, and the ground-state energy difference is lowered to a constant value.

**Summary and outlook.**—In this Letter, we presented an in-depth study of ground-state string behavior in a  $\mathbb{Z}_2$  lattice gauge theory with Ising matter in the

presence of two static charges. We outlined the role of the plaquette term in stabilizing strings in the confined phase. We provided a mapping to a free-fermionic chain in the presence of a weak magnetic field. Our findings can be readily tested on superconducting-qubit quantum computers such as the one used in the experiment [55]. Several possible generalizations will be the subject of future research. Novel phenomena can arise when considering different types of matter fields, such as fermions, or models with different global or gauge symmetries. Different lattice geometries may also have a significant impact on the nature of string breaking, especially those relevant to Rydberg-atom realizations [38].

**Acknowledgments.**—U.B. acknowledges support from the Israel Academy of Sciences and Humanities through the Excellence Fellowship for International Postdoctoral Researchers. S.M. is supported by Vetenskapsrådet (grant number 2021-03685) and acknowledges support provided by Nordita. J.C.H. acknowledges funding by the Max Planck Society, the Deutsche Forschungsgemeinschaft (DFG, German Research Foundation) under Germany’s Excellence Strategy – EXC-2111 – 390814868, and the European Research Council (ERC) under the European Union’s Horizon Europe research and innovation program (Grant Agreement No. 101165667)—ERC Starting Grant QuSiGauge. This work is part of the Quantum Computing for High-Energy Physics (QC4HEP) working group.

---

\* [jad.halimeh@physik.lmu.de](mailto:jad.halimeh@physik.lmu.de)

- [1] S. Weinberg, *The Quantum Theory of Fields*, Vol. 2: Modern Applications (Cambridge University Press, 1995).
- [2] C. Gattringer and C. Lang, *Quantum Chromodynamics on the Lattice: An Introductory Presentation*, Lecture Notes in Physics (Springer Berlin Heidelberg, 2009).
- [3] R. Ellis, W. Stirling, and B. Webber, *QCD and Collider Physics*, Cambridge Monographs on Particle Physics, Nuclear Physics and Cosmology (Cambridge University Press, 2003).
- [4] K. G. Wilson, Confinement of quarks, *Phys. Rev. D* **10**, 2445 (1974).
- [5] F. J. Wegner, Duality in generalized Ising models and phase transitions without local order parameters, *Journal of Mathematical Physics* **12**, 2259 (1971), [https://pubs.aip.org/aip/jmp/article-pdf/12/10/2259/19106483/2259\\_1\\_online.pdf](https://pubs.aip.org/aip/jmp/article-pdf/12/10/2259/19106483/2259_1_online.pdf).
- [6] J. B. Kogut, An introduction to lattice gauge theory and spin systems, *Rev. Mod. Phys.* **51**, 659 (1979).
- [7] X. Wen, *Quantum Field Theory of Many-Body Systems: From the Origin of Sound to an Origin of Light and Electrons: From the Origin of Sound to an Origin of Light and Electrons*, Oxford Graduate Texts (OUP Oxford, 2004).
- [8] H. Bernien, S. Schwartz, A. Keesling, H. Levine, A. Omran, H. Pichler, S. Choi, A. S. Zibrov, M. Endres, M. Greiner, V. Vuletić, and M. D. Lukin, Probing many-body dynamics on a 51-atom quantum simulator, *Nature* **551**, 579 (2017).
- [9] F. M. Surace, P. P. Mazza, G. Giudici, A. Leroze, A. Gambassi, and M. Dalmonte, Lattice gauge theories and string dynamics in Rydberg atom quantum simulators, *Phys. Rev. X* **10**, 021041 (2020).
- [10] G.-X. Su, H. Sun, A. Hudomal, J.-Y. Desaulles, Z.-Y. Zhou, B. Yang, J. C. Halimeh, Z.-S. Yuan, Z. Papić, and J.-W. Pan, Observation of many-body scarring in a Bose-Hubbard quantum simulator, *Phys. Rev. Res.* **5**, 023010 (2023).
- [11] J.-Y. Desaulles, D. Banerjee, A. Hudomal, Z. Papić, A. Sen, and J. C. Halimeh, Weak Ergodicity Breaking in the Schwinger Model, arXiv preprint (2022), [arXiv:2203.08830 \[cond-mat.str-el\]](https://arxiv.org/abs/2203.08830).
- [12] J.-Y. Desaulles, A. Hudomal, D. Banerjee, A. Sen, Z. Papić, and J. C. Halimeh, Prominent quantum many-body scars in a truncated Schwinger model [10.48550/ARXIV.2204.01745](https://arxiv.org/abs/2204.01745) (2022).
- [13] E. A. Martinez, C. A. Muschik, P. Schindler, D. Nigg, A. Erhard, M. Heyl, P. Hauke, M. Dalmonte, T. Monz, P. Zoller, and R. Blatt, Real-time dynamics of lattice gauge theories with a few-qubit quantum computer, *Nature* **534**, 516 (2016).
- [14] N. Klco, E. F. Dumitrescu, A. J. McCaskey, T. D. Morris, R. C. Pooser, M. Sanz, E. Solano, P. Lougovski, and M. J. Savage, Quantum-classical computation of Schwinger model dynamics using quantum computers, *Phys. Rev. A* **98**, 032331 (2018).
- [15] F. Görg, K. Sandholzer, J. Minguzzi, R. Desbuquois, M. Messer, and T. Esslinger, Realization of density-dependent Peierls phases to engineer quantized gauge fields coupled to ultracold matter, *Nat. Phys.* **15**, 1161 (2019).
- [16] C. Schweizer, F. Grusdt, M. Berngruber, L. Barbiero, E. Demler, N. Goldman, I. Bloch, and M. Aidelsburger, Floquet approach to  $\mathbb{Z}_2$  lattice gauge theories with ultracold atoms in optical lattices, *Nat. Phys.* **15**, 1168 (2019).
- [17] A. Mil, T. V. Zache, A. Hegde, A. Xia, R. P. Bhatt, M. K. Oberthaler, P. Hauke, J. Berges, and F. Jendrzejewski, A scalable realization of local U(1) gauge invariance in cold atomic mixtures, *Science* **367**, 1128 (2020).
- [18] B. Yang, H. Sun, R. Ott, H.-Y. Wang, T. V. Zache, J. C. Halimeh, Z.-S. Yuan, P. Hauke, and J.-W. Pan, Observation of gauge invariance in a 71-site Bose-Hubbard quantum simulator, *Nature* **587**, 392 (2020).
- [19] Z. Wang, Z.-Y. Ge, Z. Xiang, X. Song, R.-Z. Huang, P. Song, X.-Y. Guo, L. Su, K. Xu, D. Zheng, and H. Fan, Observation of emergent  $\mathbb{Z}_2$  gauge invariance in a superconducting circuit, *Phys. Rev. Research* **4**, L022060 (2022).
- [20] Z.-Y. Zhou, G.-X. Su, J. C. Halimeh, R. Ott, H. Sun, P. Hauke, B. Yang, Z.-S. Yuan, J. Berges, and J.-W. Pan, Thermalization dynamics of a gauge theory on a quantum simulator, *Science* **377**, 311 (2022).
- [21] H.-Y. Wang, W.-Y. Zhang, Z. Yao, Y. Liu, Z.-H. Zhu, Y.-G. Zheng, X.-K. Wang, H. Zhai, Z.-S. Yuan, and J.-W. Pan, Interrelated thermalization and quantum criticality in a lattice gauge simulator, *Phys. Rev. Lett.* **131**, 050401 (2023).
- [22] W.-Y. Zhang, Y. Liu, Y. Cheng, M.-G. He, H.-Y. Wang, T.-Y. Wang, Z.-H. Zhu, G.-X. Su, Z.-Y. Zhou, Y.-G. Zheng, H. Sun, B. Yang, P. Hauke, W. Zheng, J. C. Halimeh, Z.-S. Yuan, and J.-W. Pan, Observation of microscopic confinement dynamics by a tunable topological  $\theta$ -angle, *Nature Physics* [10.1038/s41567-024-02702-x](https://doi.org/10.1038/s41567-024-02702-x)

- (2024).
- [23] Z.-H. Zhu, Y. Liu, G. Lagnese, F. M. Surace, W.-Y. Zhang, M.-G. He, J. C. Halimeh, M. Dalmonte, S. C. Morampudi, F. Wilczek, Z.-S. Yuan, and J.-W. Pan, Probing false vacuum decay on a cold-atom gauge-theory quantum simulator, (2024), [arXiv:2411.12565](https://arxiv.org/abs/2411.12565) [[cond-mat.quant-gas](https://arxiv.org/abs/2411.12565)].
- [24] M. Dalmonte and S. Montangero, Lattice gauge theory simulations in the quantum information era, *Contemporary Physics* **57**, 388 (2016), <https://doi.org/10.1080/00107514.2016.1151199>.
- [25] M. C. Bañuls, R. Blatt, J. Catani, A. Celi, J. I. Cirac, M. Dalmonte, L. Fallani, K. Jansen, M. Lewenstein, S. Montangero, C. A. Muschik, B. Reznik, E. Rico, L. Tagliacozzo, K. Van Acoleyen, F. Verstraete, U.-J. Wiese, M. Wingate, J. Zakrzewski, and P. Zoller, Simulating lattice gauge theories within quantum technologies, *The European Physical Journal D* **74**, 165 (2020).
- [26] E. Zohar, J. I. Cirac, and B. Reznik, Quantum simulations of lattice gauge theories using ultracold atoms in optical lattices, *Rep. Prog. Phys.* **79**, 014401 (2015).
- [27] Y. Alexeev, D. Bacon, K. R. Brown, R. Calderbank, L. D. Carr, F. T. Chong, B. DeMarco, D. Englund, E. Farhi, B. Fefferman, A. V. Gorshkov, A. Houck, J. Kim, S. Kimmel, M. Lange, S. Lloyd, M. D. Lukin, D. Maslov, P. Maunz, C. Monroe, J. Preskill, M. Roetteler, M. J. Savage, and J. Thompson, Quantum computer systems for scientific discovery, *PRX Quantum* **2**, 017001 (2021).
- [28] M. Aidelsburger, L. Barbiero, A. Bermudez, T. Chanda, A. Dauphin, D. González-Cuadra, P. R. Grzybowski, S. Hands, F. Jendrzejewski, J. Jünemann, G. Juzeliūnas, V. Kasper, A. Piga, S.-J. Ran, M. Rizzi, G. Sierra, L. Tagliacozzo, E. Tirrito, T. V. Zache, J. Zakrzewski, E. Zohar, and M. Lewenstein, Cold atoms meet lattice gauge theory, *Philosophical Transactions of the Royal Society A: Mathematical, Physical and Engineering Sciences* **380**, 20210064 (2022).
- [29] E. Zohar, Quantum simulation of lattice gauge theories in more than one space dimension—requirements, challenges and methods, *Philos. Trans. Royal Soc. A* **380**, 20210069 (2022), [arXiv:2106.04609](https://arxiv.org/abs/2106.04609) [[quant-ph](https://arxiv.org/abs/2106.04609)].
- [30] N. Klco, A. Roggero, and M. J. Savage, Standard model physics and the digital quantum revolution: thoughts about the interface, *Reports on Progress in Physics* **85**, 064301 (2022).
- [31] C. W. Bauer, Z. Davoudi, A. B. Balantekin, T. Bhattacharya, M. Carena, W. A. de Jong, P. Draper, A. El-Khadra, N. Gemelke, M. Hanada, D. Kharzeev, H. Lamm, Y.-Y. Li, J. Liu, M. Lukin, Y. Meurice, C. Monroe, B. Nachman, G. Pagano, J. Preskill, E. Rinaldi, A. Roggero, D. I. Santiago, M. J. Savage, I. Siddiqi, G. Siopsis, D. Van Zanten, N. Wiebe, Y. Yamauchi, K. Yeter-Aydeniz, and S. Zorzetti, Quantum simulation for high-energy physics, *PRX Quantum* **4**, 027001 (2023).
- [32] A. Di Meglio, K. Jansen, I. Tavernelli, C. Alexandrou, S. Arunachalam, C. W. Bauer, K. Borras, S. Carrazza, A. Crippa, V. Croft, R. de Putter, A. Delgado, V. Dunjko, D. J. Egger, E. Fernández-Combarro, E. Fuchs, L. Funcke, D. González-Cuadra, M. Grossi, J. C. Halimeh, Z. Holmes, S. Kühn, D. Lacroix, R. Lewis, D. Lucchesi, M. L. Martinez, F. Meloni, A. Mezzacapo, S. Montangero, L. Nagano, V. R. Pascuzzi, V. Radescu, E. R. Ortega, A. Roggero, J. Schuhmacher, J. Seixas, P. Silvi, P. Spentzouris, F. Tacchino, K. Temme, K. Terashi, J. Tura, C. Tüysüz, S. Vallecorsa, U.-J. Wiese, S. Yoo, and J. Zhang, Quantum computing for high-energy physics: State of the art and challenges, *PRX Quantum* **5**, 037001 (2024).
- [33] Y. Cheng and H. Zhai, Emergent  $U(1)$  lattice gauge theory in Rydberg atom arrays, *Nature Reviews Physics* **6**, 566 (2024).
- [34] J. C. Halimeh, M. Aidelsburger, F. Grusdt, P. Hauke, and B. Yang, Cold-atom quantum simulators of gauge theories, *Nature Physics* **10.1038/s41567-024-02721-8** (2025).
- [35] U. Borla, R. Verresen, F. Grusdt, and S. Moroz, Confined phases of one-dimensional spinless fermions coupled to  $\mathbb{Z}_2$  gauge theory, *Phys. Rev. Lett.* **124**, 120503 (2020).
- [36] D. González-Cuadra, L. Tagliacozzo, M. Lewenstein, and A. Bermudez, Robust topological order in fermionic  $\mathbb{Z}_2$  gauge theories: From aharonov-bohm instability to soliton-induced deconfinement, *Phys. Rev. X* **10**, 041007 (2020).
- [37] M. c. v. Kebrič, L. Barbiero, C. Reinmoser, U. Schollwöck, and F. Grusdt, Confinement and Mott transitions of dynamical charges in one-dimensional lattice gauge theories, *Phys. Rev. Lett.* **127**, 167203 (2021).
- [38] L. Homeier, A. Bohrdt, S. Linsel, E. Demler, J. C. Halimeh, and F. Grusdt, Realistic scheme for quantum simulation of  $\mathbb{Z}_2$  lattice gauge theories with dynamical matter in  $2 + 1d$ , *Commun. Phys.* **6**, 127 (2023).
- [39] M. Fromm, O. Philipsen, M. Spannowsky, and C. Winterowd, Simulating  $\mathbb{Z}_2$  lattice gauge theory with the variational quantum thermalizer, *EPJ Quantum Technology* **11**, 20 (2024).
- [40] M. c. v. Kebrič, J. C. Halimeh, U. Schollwöck, and F. Grusdt, Confinement in  $(1 + 1)$ -dimensional  $\mathbb{Z}_2$  lattice gauge theories at finite temperature, *Phys. Rev. B* **109**, 245110 (2024).
- [41] S. M. Linsel, A. Bohrdt, L. Homeier, L. Pollet, and F. Grusdt, Percolation as a confinement order parameter in  $\mathbb{Z}_2$  lattice gauge theories, *Phys. Rev. B* **110**, L241101 (2024).
- [42] F. F. Assaad and T. Grover, Simple fermionic model of deconfined phases and phase transitions, *Phys. Rev. X* **6**, 041049 (2016).
- [43] S. Gazit, F. F. Assaad, S. Sachdev, A. Vishwanath, and C. Wang, Confinement transition of  $\mathbb{Z}_2$  gauge theories coupled to massless fermions: Emergent quantum chromodynamics and  $SO(5)$  symmetry, *Proceedings of the National Academy of Sciences* **115**, E6987 (2018).
- [44] E. J. König, P. Coleman, and A. M. Tsvelik, Soluble limit and criticality of fermions in  $\mathbb{Z}_2$  gauge theories, *Phys. Rev. B* **102**, 155143 (2020).
- [45] A. M. Somoza, P. Serna, and A. Nahum, Self-dual criticality in three-dimensional  $\mathbb{Z}_2$  gauge theory with matter, *Phys. Rev. X* **11**, 041008 (2021).
- [46] U. Borla, S. Gazit, and S. Moroz, Deconfined quantum criticality in Ising gauge theory entangled with single-component fermions, *Phys. Rev. B* **110**, L201110 (2024).
- [47] W.-T. Xu, F. Pollmann, and M. Knap, Critical behavior of the Fredenhagen-Marcu order parameter at topological phase transitions, (2024), [arXiv:2402.00127](https://arxiv.org/abs/2402.00127) [[cond-mat.str-el](https://arxiv.org/abs/2402.00127)].
- [48] U. Borla, R. Verresen, J. Shah, and S. Moroz, Gauging the Kitaev chain, *SciPost Phys.* **10**, 148 (2021).
- [49] R. Verresen, U. Borla, A. Vishwanath, S. Moroz, and R. Thorngren, Higgs condensates are symmetry-

- protected topological phases: I. discrete symmetries, arXiv preprint arXiv:2211.01376 (2022).
- [50] T. Iadecola and M. Schechter, Quantum many-body scar states with emergent kinetic constraints and finite-entanglement revivals, *Phys. Rev. B* **101**, 024306 (2020).
- [51] A. S. Aramthottil, U. Bhattacharya, D. González-Cuadra, M. Lewenstein, L. Barbiero, and J. Zakrzewski, Scar states in deconfined  $\mathbb{Z}_2$  lattice gauge theories, *Phys. Rev. B* **106**, L041101 (2022).
- [52] J.-Y. Desaulles, T. Iadecola, and J. C. Halimeh, Mass-assisted local deconfinement in a confined  $\mathbb{Z}_2$  lattice gauge theory, (2024), arXiv:2404.11645 [cond-mat.quant-gas].
- [53] J. Mildeberger, W. Mruczkiewicz, J. C. Halimeh, Z. Jiang, and P. Hauke, Confinement in a  $\mathbb{Z}_2$  lattice gauge theory on a quantum computer, *Nature Physics* **10.1038/s41567-024-02723-6** (2025).
- [54] A. De, A. Lerose, D. Luo, F. M. Surace, A. Schuckert, E. R. Bennewitz, B. Ware, W. Morong, K. S. Collins, Z. Davoudi, A. V. Gorshkov, O. Katz, and C. Monroe, Observation of string-breaking dynamics in a quantum simulator, (2024), arXiv:2410.13815 [quant-ph].
- [55] T. A. Cochran, B. Jobst, E. Rosenberg, Y. D. Lensky, G. Gyawali, N. Eassa, M. Will, D. Abanin, R. Acharya, L. A. Beni, T. I. Andersen, M. Ansmann, F. Arute, K. Arya, A. Asfaw, J. Atalaya, R. Babbush, B. Ballard, J. C. Bardin, A. Bengtsson, A. Bilmes, A. Bourassa, J. Bovaird, M. Broughton, D. A. Browne, B. Buchea, B. B. Buckley, T. Burger, B. Burkett, N. Bushnell, A. Cabrera, J. Campero, H.-S. Chang, Z. Chen, B. Chiaro, J. Claes, A. Y. Cleland, J. Cogan, R. Collins, P. Conner, W. Courtney, A. L. Crook, B. Curtin, S. Das, S. Demura, L. D. Lorenzo, A. D. Paolo, P. Donohoe, I. Drozdov, A. Dunsworth, A. Eickbusch, A. M. Elbag, M. Elzouka, C. Erickson, V. S. Ferreira, L. F. Burgos, E. Forati, A. G. Fowler, B. Foxen, S. Ganjam, R. Gasca, Élie Genois, W. Giang, D. Gilboa, R. Gosula, A. G. Dau, D. Graumann, A. Greene, J. A. Gross, S. Habegger, M. Hansen, M. P. Harrigan, S. D. Harrington, P. Heu, O. Higgott, J. Hilton, H.-Y. Huang, A. Huff, W. J. Huggins, E. Jeffrey, Z. Jiang, C. Jones, C. Joshi, P. Juhas, D. Kafri, H. Kang, A. H. Karamlou, K. Kechedzhi, T. Khaira, T. Khattar, M. Khezri, S. Kim, P. V. Klimov, B. Kobrin, A. N. Korotkov, F. Kostritsa, J. M. Kreikebaum, V. D. Kurilovich, D. Landhuis, T. Lange-Dei, B. W. Langlely, K.-M. Lau, J. Ledford, K. Lee, B. J. Lester, L. L. Guevel, W. Y. Li, A. T. Lill, W. P. Livingston, A. Locharla, D. Lundahl, A. Lunt, S. Madhuk, A. Maloney, S. Mandrà, L. S. Martin, O. Martin, C. Maxfield, J. R. McClean, M. McEwen, S. Meeks, A. Megrant, K. C. Miao, R. Molavi, S. Molina, S. Montazeri, R. Movassagh, C. Neill, M. Newman, A. Nguyen, M. Nguyen, C.-H. Ni, M. Y. Niu, W. D. Oliver, K. Ottosson, A. Pizzuto, R. Potter, O. Pritchard, C. Quintana, G. Ramachandran, M. J. Reagor, D. M. Rhodes, G. Roberts, K. Sankaragomathi, K. J. Satzinger, H. F. Schurkus, M. J. Shearn, A. Shorter, N. Shutty, V. Shvarts, V. Sivak, S. Small, W. C. Smith, S. Springer, G. Sterling, J. Suchard, A. Szasz, A. Szein, D. Thor, M. M. Torunbalci, A. Vaishnav, J. Vargas, S. Vdovichev, G. Vidal, C. V. Heidweiller, S. Waltman, S. X. Wang, B. Ware, T. White, K. Wong, B. W. K. Woo, C. Xing, Z. J. Yao, P. Yeh, B. Ying, J. Yoo, N. Yosri, G. Young, A. Zalcman, Y. Zhang, N. Zhu, N. Zobris, S. Boixo, J. Kelly, E. Lucero, Y. Chen, V. Smelyanskiy, H. Neven, A. Gammon-Smith, F. Pollmann, M. Knap, and P. Roushan, Visualizing dynamics of charges and strings in (2+1)d lattice gauge theories, (2024), arXiv:2409.17142 [quant-ph].
- [56] G. Gyawali, T. Cochran, Y. Lensky, E. Rosenberg, A. H. Karamlou, K. Kechedzhi, J. Berndtsson, T. Westerhout, A. Asfaw, D. Abanin, R. Acharya, L. A. Beni, T. I. Andersen, M. Ansmann, F. Arute, K. Arya, N. Astrakhantsev, J. Atalaya, R. Babbush, B. Ballard, J. C. Bardin, A. Bengtsson, A. Bilmes, G. Bortoli, A. Bourassa, J. Bovaird, L. Brill, M. Broughton, D. A. Browne, B. Buchea, B. B. Buckley, D. A. Buell, T. Burger, B. Burkett, N. Bushnell, A. Cabrera, J. Campero, H.-S. Chang, Z. Chen, B. Chiaro, J. Claes, A. Y. Cleland, J. Cogan, R. Collins, P. Conner, W. Courtney, A. L. Crook, S. Das, D. M. Debroy, L. D. Lorenzo, A. D. T. Barba, S. Demura, A. D. Paolo, P. Donohoe, I. Drozdov, A. Dunsworth, C. Earle, A. Eickbusch, A. M. Elbag, M. Elzouka, C. Erickson, L. Faoro, R. Fatemi, V. S. Ferreira, L. F. Burgos, E. Forati, A. G. Fowler, B. Foxen, S. Ganjam, R. Gasca, W. Giang, C. Gidney, D. Gilboa, R. Gosula, A. G. Dau, D. Graumann, A. Greene, J. A. Gross, S. Habegger, M. C. Hamilton, M. Hansen, M. P. Harrigan, S. D. Harrington, S. Heslin, P. Heu, G. Hill, J. Hilton, M. R. Hoffmann, H.-Y. Huang, A. Huff, W. J. Huggins, L. B. Ioffe, S. V. Isakov, E. Jeffrey, Z. Jiang, C. Jones, S. Jordan, C. Joshi, P. Juhas, D. Kafri, H. Kang, T. Khaira, T. Khattar, M. Khezri, M. Kieferová, S. Kim, P. V. Klimov, A. R. Klots, B. Kobrin, A. N. Korotkov, F. Kostritsa, J. M. Kreikebaum, V. D. Kurilovich, D. Landhuis, T. Lange-Dei, B. W. Langlely, P. Laptev, K.-M. Lau, L. L. Guevel, J. Ledford, J. Lee, K. Lee, B. J. Lester, W. Y. Li, A. T. Lill, W. Liu, W. P. Livingston, A. Locharla, D. Lundahl, A. Lunt, S. Madhuk, A. Maloney, S. Mandrà, L. S. Martin, S. Martin, O. Martin, C. Maxfield, J. R. McClean, M. McEwen, S. Meeks, A. Megrant, X. Mi, K. C. Miao, A. Mieszala, S. Molina, S. Montazeri, A. Morvan, R. Movassagh, C. Neill, A. Nersisyan, M. Newman, A. Nguyen, M. Nguyen, C.-H. Ni, M. Y. Niu, W. D. Oliver, K. Ottosson, A. Pizzuto, R. Potter, O. Pritchard, L. P. Pryadko, C. Quintana, M. J. Reagor, D. M. Rhodes, G. Roberts, C. Rocque, N. C. Rubin, N. Saei, K. Sankaragomathi, K. J. Satzinger, H. F. Schurkus, C. Schuster, M. J. Shearn, A. Shorter, N. Shutty, V. Shvarts, V. Sivak, J. Skruzny, S. Small, W. C. Smith, S. Springer, G. Sterling, J. Suchard, M. Szalay, A. Szasz, A. Szein, D. Thor, M. M. Torunbalci, A. Vaishnav, S. Vdovichev, G. Vidal, C. V. Heidweiller, S. Waltman, S. X. Wang, T. White, K. Wong, B. W. K. Woo, C. Xing, Z. J. Yao, P. Yeh, B. Ying, J. Yoo, N. Yosri, G. Young, A. Zalcman, Y. Zhang, N. Zhu, N. Zobrist, S. Boixo, J. Kelly, E. Lucero, Y. Chen, V. Smelyanskiy, H. Neven, D. Kovrizhin, J. Knolle, J. C. Halimeh, I. Aleiner, R. Moessner, and P. Roushan, Observation of disorder-free localization and efficient disorder averaging on a quantum processor, (2024), arXiv:2410.06557 [quant-ph].
- [57] D. Gonzalez-Cuadra, M. Hamdan, T. V. Zache, B. Braverman, M. Kornjaca, A. Lukin, S. H. Cantu, F. Liu, S.-T. Wang, A. Keesling, M. D. Lukin, P. Zoller, and A. Bylinskii, Observation of string breaking on a (2 + 1)d Rydberg quantum simulator, (2024),

- arXiv:2410.16558 [quant-ph].
- [58] Y. Liu, W.-Y. Zhang, Z.-H. Zhu, M.-G. He, Z.-S. Yuan, and J.-W. Pan, String breaking mechanism in a lattice schwinger model simulator, (2024), arXiv:2411.15443 [cond-mat.quant-gas].
- [59] A. Crippa, K. Jansen, and E. Rinaldi, Analysis of the confinement string in  $(2 + 1)$ -dimensional quantum electrodynamics with a trapped-ion quantum computer, (2024), arXiv:2411.05628 [hep-lat].
- [60] C. Gross and W. S. Bakr, Quantum gas microscopy for single atom and spin detection, *Nat. Phys.* **17**, 1316 (2021).
- [61] J. Berges, M. P. Heller, A. Mazeliauskas, and R. Venugopalan, QCD thermalization: Ab initio approaches and interdisciplinary connections, *Rev. Mod. Phys.* **93**, 035003 (2021).
- [62] R. Verdel, F. Liu, S. Whitsitt, A. V. Gorshkov, and M. Heyl, Real-time dynamics of string breaking in quantum spin chains, *Phys. Rev. B* **102**, 014308 (2020).
- [63] R. Verdel, G.-Y. Zhu, and M. Heyl, Dynamical localization transition of string breaking in quantum spin chains, *Phys. Rev. Lett.* **131**, 230402 (2023).
- [64] A. Mallick, M. Lewenstein, J. Zakrzewski, and M. Płodzień, String breaking dynamics in Ising chain with local vibrations, (2024), arXiv:2501.00604 [quant-ph].
- [65] E. Fradkin and S. H. Shenker, Phase diagrams of lattice gauge theories with Higgs fields, *Phys. Rev. D* **19**, 3682 (1979).
- [66] S. Trebst, P. Werner, M. Troyer, K. Shtengel, and C. Nayak, Breakdown of a topological phase: Quantum phase transition in a loop gas model with tension, *Phys. Rev. Lett.* **98**, 070602 (2007).
- [67] J. Vidal, S. Dusuel, and K. P. Schmidt, Low-energy effective theory of the toric code model in a parallel magnetic field, *Phys. Rev. B* **79**, 033109 (2009).
- [68] F. Wu, Y. Deng, and N. Prokof'ev, Phase diagram of the toric code model in a parallel magnetic field, *Phys. Rev. B* **85**, 195104 (2012).
- [69] U. Schollwöck, The density-matrix renormalization group in the age of matrix product states, *Ann. Phys.* **326**, 96 (2011), january 2011 Special Issue.
- [70] I. S. Tupitsyn, A. Kitaev, N. V. Prokof'ev, and P. C. E. Stamp, Topological multicritical point in the phase diagram of the toric code model and three-dimensional lattice gauge Higgs model, *Phys. Rev. B* **82**, 085114 (2010).
- [71] W.-T. Xu, T. Rakovszky, M. Knap, and F. Pollmann, Entanglement properties of gauge theories from higher-form symmetries, *Phys. Rev. X* **15**, 011001 (2025).
- [72] F. Wu, Y. Deng, and N. Prokof'ev, Phase diagram of the toric code model in a parallel magnetic field, *Phys. Rev. B* **85**, 195104 (2012).
- [73] E. Fradkin, *Field Theories of Condensed Matter Physics*, Field Theories of Condensed Matter Physics (Cambridge University Press, 2013).
- [74] M. E. Peskin, Critical point behavior of the Wilson loop, *Physics Letters B* **94**, 161 (1980).
- [75] J. Hauschild and F. Pollmann, Efficient numerical simulations with Tensor Networks: Tensor Network Python (TeNPy), *SciPost Phys. Lect. Notes* , 5 (2018).
- [76] J. Hauschild, J. Unfried, S. Anand, B. Andrews, M. Bintz, U. Borla, S. Divic, M. Drescher, J. Geiger, M. Hefel, K. Hémerly, W. Kadow, J. Kemp, N. Kirchner, V. S. Liu, G. Möller, D. Parker, M. Rader, A. Romén, S. Scalet, L. Schoonderwoerd, M. Schulz, T. Soejima, P. Thoma, Y. Wu, P. Zechmann, L. Zweng, R. S. K. Mong, M. P. Zaletel, and F. Pollmann, Tensor network Python (TeNPy) version 1, *SciPost Phys. Codebases* , 41 (2024).